ISSN 0036-0244, Russian Journal of Physical Chemistry A, 2019, Vol. 93, No. 11, pp. 2226–2232. © Pleiades Publishing, Ltd., 2019.

STRUCTURE OF MATTER AND QUANTUM CHEMISTRY

An Ab-initio Study of Structural and Electronic Properties of CaTe under High Pressure

Cihan Kürkçü[a,*]

[a] *Department of Electronics and Automation, Ahi Evran University, Kirsehir, Turkey*

**e-mail: ckurkcu@ahievran.edu.tr*

Received September 21, 2018; revised November 15, 2018; accepted January 15, 2019

Abstract—The crystal structure of the CaTe compound is studied up to 150 GPa under high hydrostatic pressure using the density functional theory (DFT) with the generalized gradient approximation (GGA). Pressure-volume relationships, structural transitions and electronic properties in CaTe compound are investigated using Siesta method. CaTe crystallizes in the NaCl-type (B1) structure (space group: $Fm\bar{3}m$) at ambient conditions, and transforms to CsCl-type (B2) structure (space group: $Pm\bar{3}m$) at high pressure. This transformation is based on a intermediate state with space group $R\bar{3}m$. Moreover, the electronic band structure of the B1 and B2 structures of CaTe have been calculated. According to this calculation, obtained band gap values are in good agreement with the values reported in the literature.

Keywords: CaTe, ab-initio, intermediate state, phase transition

DOI: 10.1134/S0036024419110165

INTRODUCTION

Under high pressure, alkaline earth chalcogenides such as CaO, CaS, CaSe, and CaTe are closed-shell ionic systems that crystallize in NaCl-type (B1) structure at ambient conditions and have technological importance in many applications, from catalysis to microelectronics [1–5], as well as in the field of luminescent devices [6–8]. X-ray diffraction studies of CaTe under high pressure have revealed that this compound undergoes first order phase transition from six-fold coordinated B1 structure to the eight-fold coordinated B2 structure at 33 GPa [9]. Pressure–volume relationships and structural phase transitions in CaTe are also investigated by X-ray diffraction method at high pressure [10].

Some basic properties of CaTe, such as changes in band gap under increasing pressure, are still unknown. Therefore, in order to understand some physical properties of this compound, it is necessary to study its electronic structure in detail. A characteristic feature of the electronic band structure of CaTe compound is the absence of *d* electrons in the valence band. There is a lack of knowledge in the literature for calcium chalcogenides among the alkaline earth chalcogenides. Therefore, in order to fully utilize these materials for new devices, the structural and electronic properties of these compounds should be investigated in more detail.

For this reason, the aim of this study is to provide a comparative study of structural and electronic properties under high pressure using Siesta method, which completes existing experimental and theoretical studies on CaTe. For this material, obtained results yield the following sequence $Fm\bar{3}m \rightarrow Pm\bar{3}m$ which is compatible with the other studies. Additionally it is also suggested that the $Pm\bar{3}m$ phase of this material proceeds through a intermediate state with space group $R\bar{3}m$ expressed as CaTe-(a). In addition, as a result of rigorous research, it is thought that the intermediate state obtained for the $Pm\bar{3}m$ phase of CaTe is first obtained in this study.

METHOD

The structural and electronic properties of the cubic NaCl-type structure of CaTe are investigated using the ab initio method in the framework of density functional theory. The SIESTA [11] package program is used as the ab-initio code in the study. Approach GGA [12] is applied and parameters of the Perdew-Burke-Ernzerhof (PBE) exchange-correlation function are entered into the calculations with "double ζ (DZ) basis set." Troullier-Martins' norm-protective pseudo-potential [13] is used for electronic band structure, total and partial density of state calculations.

Cut off energy at work is sufficient as 300 Ryd. In order to calculate the relation between the energy- volume, the unit cells of the crystal structures are utilized for B1 and B2 structures.For Brillouin region integra-

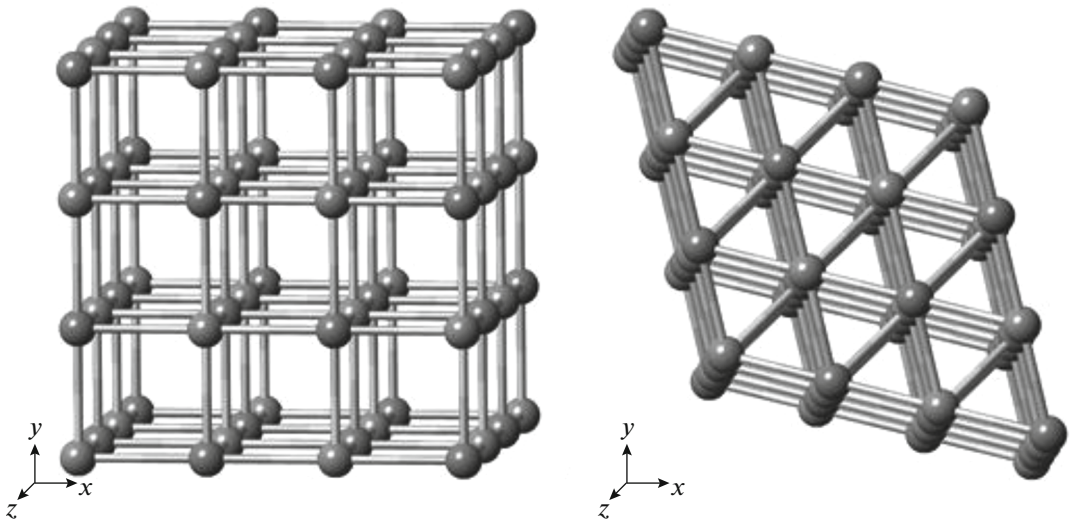

Fig. 1. Crystal structures of CaTe: B1 structure (left) at zero pressure and B2 structure (right) at 120 GPa.

tion, 8 × 8 × 8 Monkhorst-Pack (MP) mesh [14] were used for both $Fm\bar{3}m$ and $Pm\bar{3}m$ phases. Simulation cells are constructed from 64 atoms under periodic bond conditions using a 2 × 2 × 2 supercell. Pressure is gradually increased by 10 GPa by applying Parrinello-Rahman technique to the system. The KPLOT [15] program and the RGS [16] algorithm are used to analyze each simulation step. They give detailed information about the space group, atomic positions and lattice parameters of an analyzed structure. MD time step was 1.0 fs. In addition, the Crystalmaker program is used to visualize phase transformation and its mechanism.

Table 1. Transition pressures (P_T), lattice lengths (a, b, and c), bulk modulus (B_0) and derivative values of bulk modulus (B_0') for $Fm\bar{3}m$ and $Pm\bar{3}m$ phases of CaTe

Phases	P_T, GPa	$a = b = c$, Å	B_0, GPa	B_0'	References
$Fm\bar{3}m$	0	6.4430	60.67	4.03	This study
		6.2310	45.40	4.20	[19]
		6.3960	39.60		[3]
		6.2080	44.03		[3]
		6.4140	43.26	3.08	[20]
		6.3480	41.80	4.30	[9]
		6.3560	42.00	5.00	[10]
		6.2550	50.69	4.36	[5]
$Pm\bar{3}m$	33.00	3.2624	70.75	4.40	This study
	26.50				[2]
	27.00	3.7990	50.20	4.20	[19]
	27.50				[21]
	30.41	3.9300	38.78	3.80	[3]
	31.58	3.8100	49.06	4.80	[3]
	34.50				[4]
	30.20	3.9400	42.60	3.32	[20]
	33.20		50.05	4.15	[1]
	33.00	3.9310	41.80	4.30	[9]
	35.00				[10]

RESULTS AND DISCUSSION

Using the KPLOT program, the structure of CaTe at each applied pressure value is analyzed, and it is observed that the cubic structure is preserved up to 120 GPa. We observed that at 120 GPa it converted from cubic B1 structure to another cubic B2 structure. These main structures we have obtained are shown in Fig. 1, and the transition pressures, lattice parameters, bulk modulus and derivate of bulk modulus of these structure are given in Table 1 in comparison with other theoretical and experimental studies.

The predicted transition pressure values in constant pressure molecular dynamics simulations are often higher than those obtained from experimental results. This is because the systems are faced with a remarkable energy barrier when passing from one phase to another. The simulated systems should pass this energy barrier in order to undergo phase transition. It will therefore require higher pressure. So the next step is to take energy–volume calculations to study the stability of CaTe's high-pressure phases. The calculated total energy–volume relations are fitted to the 3rd degree Birch-Murnaghan state equation given in following equation:

$$P = 1.5B_0[(V/V_0)^{-7/3} - (V/V_0)^{-5/3}]x \times \{1 + 0.75(B_0' - 4)[(V/V_0)^{-2/3} - 1]\}, \quad (1)$$

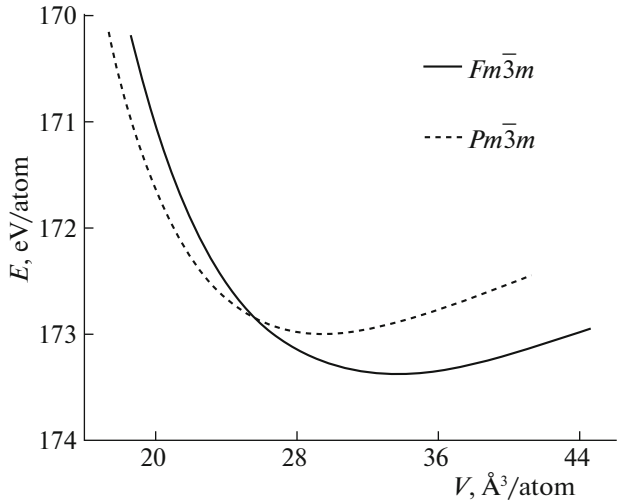

Fig. 2. Energy–volume graph of the main structural phases of the CaTe compound.

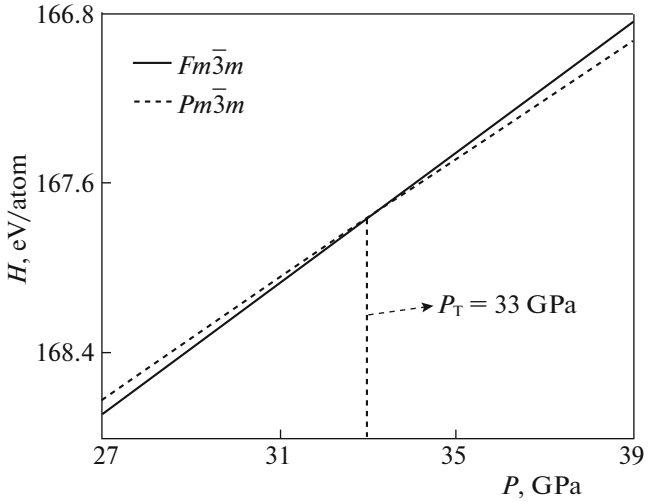

Fig. 3. Enthalpy graph for the stable phases of CaTe as the function of the pressure.

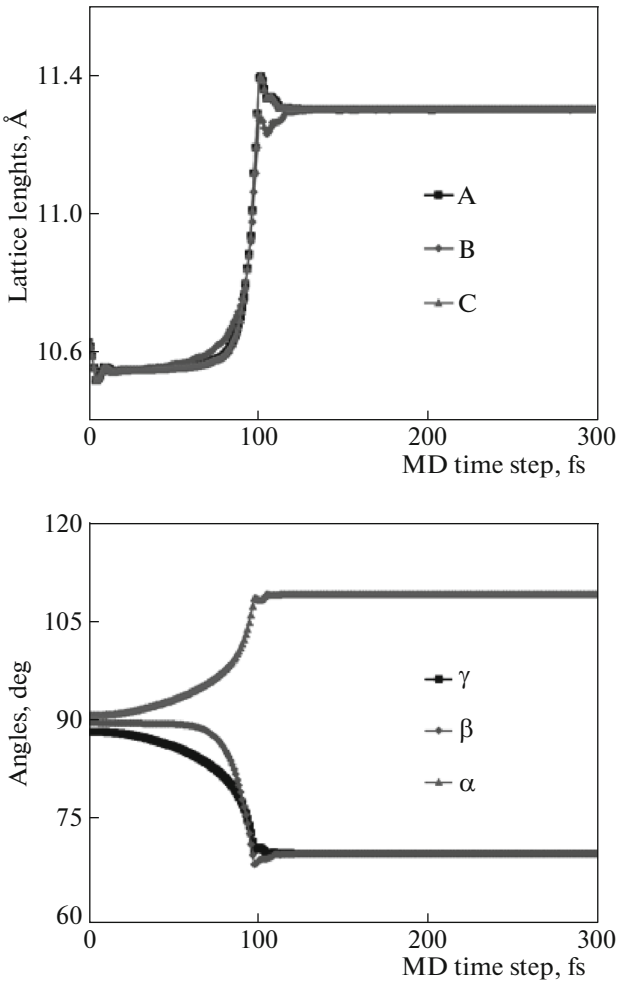

Fig. 4. Lattice vector lengths and the variation of the angles between these vectors of CaTe at 120 GPa.

where P is the pressure, V is the volume, V_0, B_0, and B_0' are the volume, bulk modulus and derivate of bulk modulus at zero pressure, respectively [17, 18], and shown in Fig. 2.

We used Gibbs free energy to determine which phase is thermodynamically stable at the given pressure and temperature. Gibbs free energy is as given in following equation:

$$G = E_{tot} + PV - TS, \quad (2)$$

where E, P, V, and S are total energy, pressure, volume and entropy, respectively. The theoretical work we have done was achieved at 0 K temperature. So the "TS" term was neglected. Thus, the Gibbs free energy G equals the enthalpy given in equation:

$$H = E_{tot} + PV, \quad (3)$$

where $P = -\partial E_{tot}/\partial V$. Enthalpy calculations usually give transition pressures that are consistent with experimental results. The intersection of two enthalpy curves shows the phase transition involving the pressure between these two phases. The enthalpy curve is plotted in Fig. 3 for the obtained phases of CaTe as a function of the pressure to determine the transition pressure. Energy–volume data are used for drawing the enthalpy curve. As can be seen from Fig. 3, the transition pressure between the B1 and B2 structures of the CaTe was obtained about 33 GPa. This result is in good agreement with experimental result [9, 10].

In order to explain the mechanism of the phase transitions, the lengths of the lattice vectors of the simulation cell and the changes in the angles between these vectors according to the simulation steps were examined. These vectors are denoted A, B, and C along the [100], [010], and [001] directions, respec-

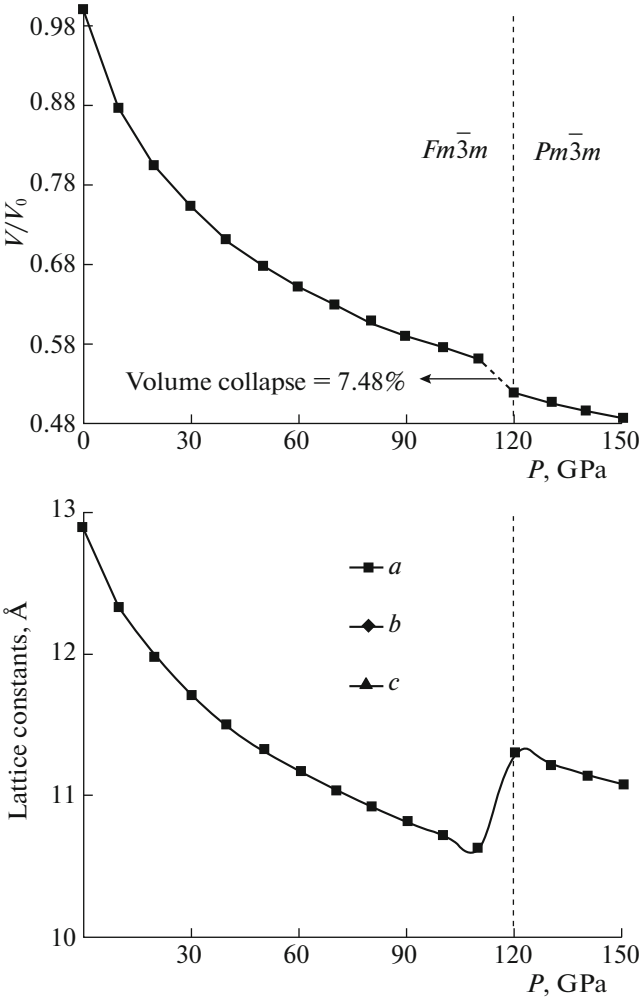

Fig. 5. The graph of the change of simulation cell volume and lattice constant as function of the pressure.

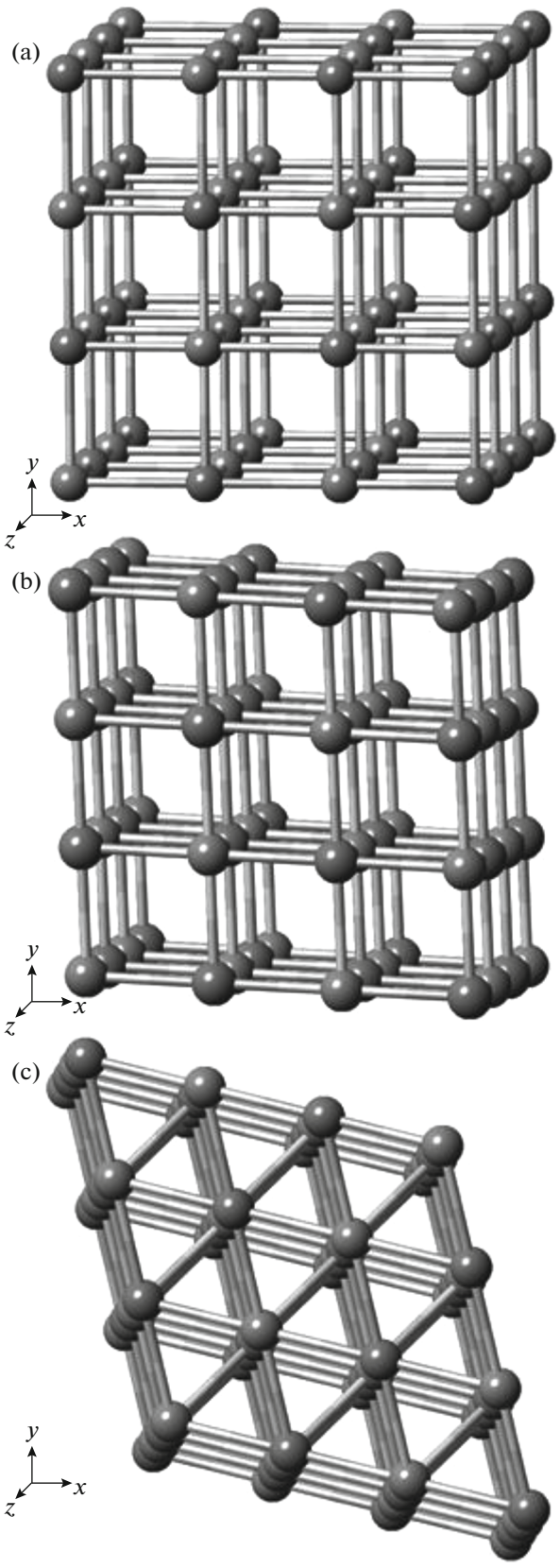

Fig. 6. Formation of CsCl (B2) structure at 120 GPa.

tively. The angle between A and B vectors, the angle between A and C vectors and the angle between A and C vectors are expressed by γ, β, and α, respectively. The lengths of the lattice vectors and the variation of the angles between these vectors according to the simulation steps are shown in Fig. 4 for 120 GPa. As shown in Fig. 4, the A, B, and C lengths remain constant up to about 100 fs. The A, B, and C lengths start to increase at around 100 fs and after reaching 11.3 Å, they remain unchanged throughout the simulation. The α, β, and γ angles also experience small changes up to about 100 fs. As the β and γ angles decrease at about 69°, α angle reaches 110° and after 100 fs, they remain constant throughout the simulation.

To determine the thermodynamic nature of the phase transition of B1 → B2 in CaTe, pressure–volume and pressure–lattice constants relations are plotted in Fig. 5. At 120 GPa the B2 type structure is characterized. This finding suggests that the first-order phase transition from B1- to B2-type structure is

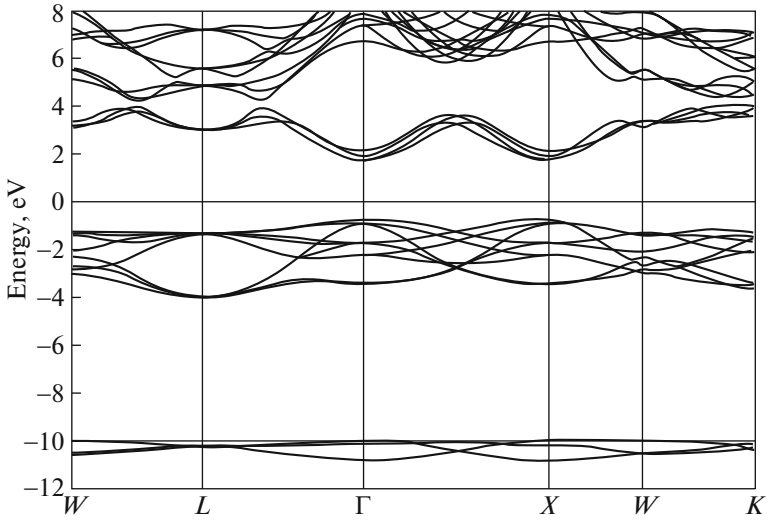

Fig. 7. Band structure for NaCl (B1) structure.

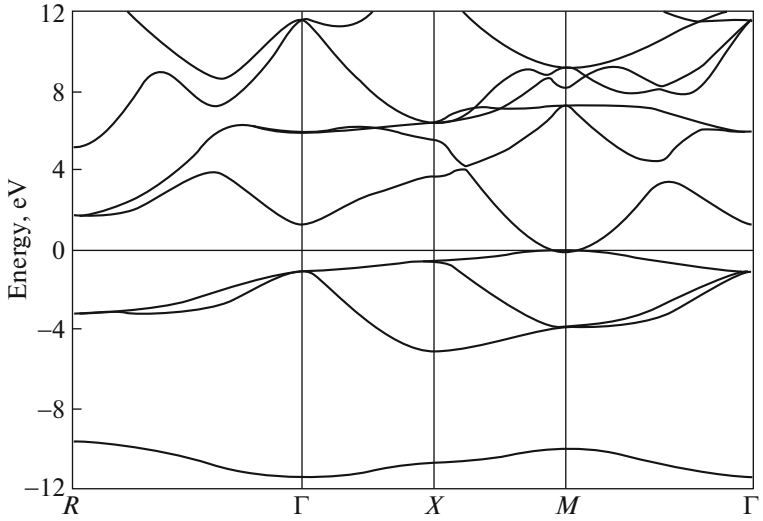

Fig. 8. Band structure for CsCl (B2) structure.

between 110 and 120 GPa. After that, pressure is increased up to 150 GPa to see how the B2 structure would respond, but we could not find any other phase transitions. As can be seen from Fig. 5, the volume and lattice constants have significantly changed when the pressure is increased from 110 to 120 GPa. The reason for this change is that at 120 GPa, the $Fm\bar{3}m$ phase turns into the $Pm\bar{3}m$ one. The collapse in the value of volume during this transformation shows us that the phase transition is first order.

Each MD time step of the B2 structure is analyzed in detail by the KPLOT program to determine whether there are any intermediate states during this phase change at 120 GPa. As a result of the analysis, the $Pm\bar{3}m$ phase of CaTe is transformed into the rhombohedral structure with space group $R\bar{3}m$ at 55th step, and then the cubic structure with space group $Pm\bar{3}m$ at 97st step. The lattice constants of this obtained rhombohedral structure are $a = 3.6385$, $b = 3.6385$, $c = 3.6385$. The formation of the this cubic B2 structure is shown in Fig. 6.

The calculated electronic band structures of CaTe are given in Figs. 7 and 8 for B1 and B2 structures, respectively. The density of state curves calculated for structures B1 and B2 are given in Figs. 9 and 10, respectively, along high symmetry directions and shown at the level of Fermi energy as a function of the energy. The Fermi energy level is set to 0 eV. The symmetry points are chosen as W–L–Γ–X–W–K for the B1 phase and R–Γ–X–M–Γ for the B2 phase. As seen from the electronic band structure graphs, the valence band is located below the Fermi energy level and the transmission band is located on the top. The obtained

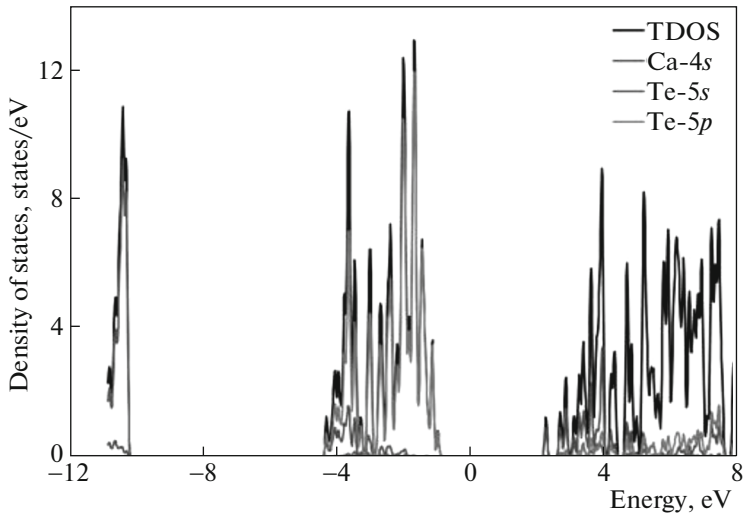

Fig. 9. Density of states in NaCl (B1) structure.

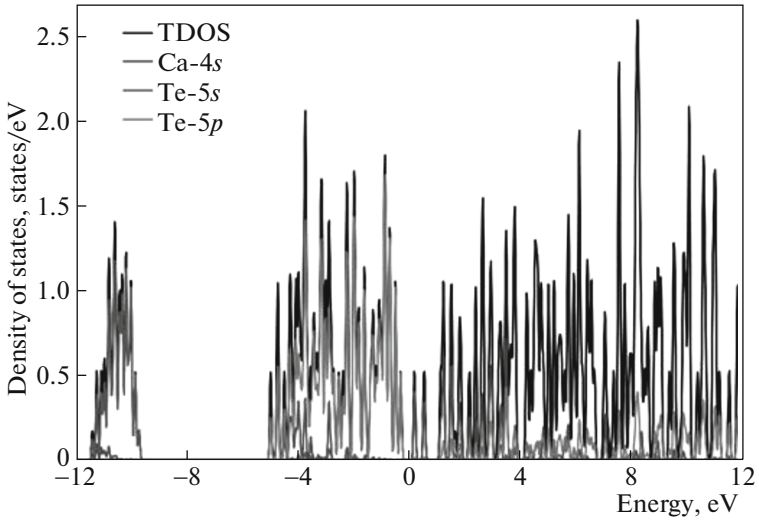

Fig. 10. Density of states in CsCl (B2) structure.

results show that CaTe at 0 GPa corresponds to a direct band transition with a band gap of about 2.48 eV [2, 3], because the maximum of the valence band and the minimum of the conduction band are at the same symmetry point [Γ]. When the increasing pressure is applied to the B1 structure of CaTe, a transformation to the B2 structure was obtained. CaTe with B2 structure is a conductor [2, 3]. In our case the transition to the metallic state occurs only after structural transformation. With overlapping of the conduction and the valence bands, the insulator–metal transformation occurs.

It is also calculated the partial density of states (PDOS) to obtain further information about the electronic nature of CaTe and depicted in Figs. 9 and 10. It can be seen from Fig. 9 that the largest contribution came from Te-5*p* states between 0 and –5 eV and from Ca-4*s* between 0 and 5 eV for B1 structure.

CONCLUSION

In the present study, the structural characterization, the electronic properties and high pressure induced phase transition in CaTe is investigated using an ab initio molecular dynamics simulations. The most relevant conclusions are summarized as follows:

(i) the calculated ground state properties of this compound at ambient pressure are comparable to the available experimental and theoretical data;

(ii) first-order phase transitions for CaTe are proposed;

(iii) the band structure calculations reveal that the cubic B1 structure (space group: $Fm\bar{3}m$) of CaTe is a

direct band gap semiconductor while another cubic structure (space group: $Pm\bar{3}m$) of CaTe is a metal.

REFERENCES

1. K. Kholiya, Phys. B: Condens. Matter **405**, 2683 (2010).
2. S. Boucenna et al., Comput. Mater. Sci. **68**, 325 (2013).
3. Z. Charifi et al., J. Phys.: Condens. Matter **17**, 4083 (2005).
4. P. K. Jha and S. P. Sanyal, Phys. Status Solidi B **212**, 241 (1999).
5. H. Khachai et al., Phys. Proc. **2**, 921 (2009).
6. S. Asano, N. Yamashita, and Y. Nakao, Phys. Status Solidi B **89**, 663 (1978).
7. Y. Nakanishi et al., Appl. Surf. Sci. **65**, 515 (1993).
8. R. Pandey and S. Sivaraman, J. Phys. Chem. Solids **52**, 211 (1991).
9. H. Luo et al., Phys. Rev. B **50**, 16232 (1994).
10. H. Zimmer, H. Winzen, and K. Syassen, Phys. Rev. B **32**, 4066 (1985).
11. P. Ordejón, E. Artacho, and J. M. Soler, Phys. Rev. B **53**, R10441 (1996).
12. J. P. Perdew, K. Burke, and M. Ernzerhof, Phys. Rev. Lett. **77**, 3865 (1996).
13. N. Troullier and J. L. Martins, Phys. Rev. B **43**, 1993 (1991).
14. H. J. Monkhorst and J. D. Pack, Phys. Rev. B **13**, 5188 (1976).
15. R. Hundt et al., J. Appl. Crystallogr. **32**, 413 (1999).
16. A. Hannemann et al., J. Appl. Crystallogr. **31**, 922 (1998).
17. F. Birch, Phys. Rev. **71**, 809 (1947).
18. F. Murnaghan, Proc. Nat. Acad. Sci. U. S. A. **30**, 244 (1944).
19. P. Cortona and P. Masri, J. Phys.: Condens. Matter **10**, 8947 (1998).
20. R. Khenata et al., Phys. B (Amsterdam, Neth.) **371**, 12 (2006).
21. J. Majewski and P. Vogl, Phys. Rev. B **35**, 9666 (1987).